Simple Efficiency Maximizer for an Adjustable Frequency Induction Motor Drive

Julio C. Moreira, *Member, IEEE,* Thomas A. Lipo, *Fellow, IEEE,* and Vladimir Blasko

Abstract—**A new method of efficiency maximization that utilizes sensing of the third-harmonic component of air gap flux is proposed. This signal is used to determine the resulting instantaneous position of the fundamental component of the air gap flux and, consequently, the torque- and flux-producing components of the stator current. In addition, the third harmonic signal is also used to determine the rotor speed. Hence, the output power of the machine can be calculated with only a single sensor wire attached to the neutral point of the machine. The flux-producing component can now be readily adjusted to produce the minimum input power for a fixed amount of output power (fixed speed).**

I. Introduction

IT IS WELL KNOWN that of the total electrical consumption of about $1700 \cdot 10^9$ kW · hr in the United States, motors consume about $1100 \cdot 10^9$ kW · hr, or 65% of the total. In the industrial sector alone, motors account for a whopping 76% [1]. Although the efficiency of electrical machinery has been on the rise, the efficiency of squirrel-cage induction motors range roughly from 78 to 92% for machines rated between 1 and 100 hp, suggesting that substantial energy savings remain to be achieved. There are estimated to be over 50 million motors in use in the industrial and commercial sectors of the United States of which 1 million are greater than 5 hp [1], [2]. There are also estimated to be over 7500 classifications of induction motors in the size range between 5 and 500 hp [2].

The losses in induction machines are typically divided into a) stator copper loss, b) rotor copper loss, c) iron losses, d) stray losses and e) friction and windage. The stator and rotor copper loss and iron plus stray losses are roughly equal and total about 90% of the total motor losses, with e) accounting for the remaining 10%. These loss distributions change when the machine is supplied from an inverter due to the presence of harmonic components in the voltage and current. In this instance, the stray load losses will increase and can become a significant part of the total loss, depending on the nature of the harmonic spectrum. A good induction machine design will dictate that operation around nominal operating conditions correspond to high efficiencies because a favorable balance between copper and iron losses is achieved. When the machine operates at lower loads or at nonrated speeds, however, its efficiency decreases due to the unbalance between the two main loss components, with the iron losses dominating at light loads. Energy can thus be saved in conventional induction motor constant speed applications when load conditions change widely by decreasing the motor flux with load, thereby reducing the iron losses at the expense of increasing the copper losses [3]. Unfortunately, most constant speed loads do not vary appreciably with time. In addition, the cost of the controller used to adjust the motor flux [4] is expensive; therefore, energy savings can only rarely be realized in fixed-frequency conventional applications.

Electrical machine static drive systems, on the other hand, inherently involve varying load demands. Such drives play an increasingly important role in many industrial, transportation, and residential applications. This role is expected to become much more evident in a very short time, with some studies showing that by the year 2000, the majority of the all energy produced in the United States will be controlled by power semiconductors [5]. Typical among such applications are compressors, pumps, fans, and blowers, including such important applications as air conditioners and heat pumps. In such cases, improvement in operating efficiency is possible at a much more attractive price since the controller used to develop the optimum flux condition is derived from the same converter used to vary the speed of the drive. In these applications, the cost of the inverter is already justified on the basis of its energy-saving impact on the load, for example, eliminating vanes to control the flow of air in a refrigeration system. Hence, additional savings in operating the motor at an optimal condition comes at a minimal expense.

Although it is not as significant as constant speed loads, energy losses in electrical drives are also a major consumer of electrical energy. According to Kirschen et al. [6], [7] a 40% reduction in losses can be achieved at 25% load throughout the speed range. For a typical 500-hp machine, this reduction of losses, at a cost of energy of \$0.05/kW · hr, represents an annual savings of about \$7000. Hence, efficiency maximization holds the promise of saving large amounts of wasted electrical energy.

A controller for saving energy in an induction motor drive has already been reported [7]. However, such controllers assume the presence of a field-oriented control system in which both the motor torque and speed are accurately sensed

Paper IPCSD 91-27, approved by the Industrial Drives Committee of the IEEE Industry Applications Society for presentation at the 1989 Industry Applications Society Annual Meeting, San Diego, CA, October 1–5. Manuscript released for publication March 1, 1989. This work was supported by the Wisconsin Electric Machines and Power Electronics Consortium.

J. C. Moreira is with Whirlpool Corporation, Benton Harbor, MI 49022.

T. A. Lipo is with the Department of Electrical and Computer Engineering, University of Wisconsin, Madison, WI 53706-1691.

V. Blasko is with Otis Research and Development Center, Farmington, CT 06932.

IEEE Log Number 9100926.

0093-9994/91/0900-0940$01.00

and/or controlled. Since the stator current is inherently resolved into its flux- and torque-producing components, the motor flux can be readily varied, whereas the torque and speed are maintained constant. Implementation of this principle in a "general-purpose" induction motor drive, however, presents a much more difficult problem since the torque is not directly controlled, and the speed is not measured. Such drives constitute the vast majority of ac motor drives in industry servicing square law load torque applications such as fans and blowers. The key to a practical implementation of an efficiency maximizer for such drives clearly hinges on developing a simple method of measuring torque and speed. Such a method could then be incorporated into any existing commercial "general-purpose" drive, which is typically operated "open loop," insofar as an external speed loop is concerned.

For this purpose, an innovative technique to determine the resulting instantaneous position of the fundamental component of the air gap flux is proposed using the third harmonic component of the stator phase voltage. This signal is used to determine the resulting instantaneous spatial position of the fundamental component of the air gap flux and, consequently, the torque and flux producing components of stator current. In addition, the third harmonic signal is also used to determine the rotor speed. The output power of the machine can thereby be calculated with the addition of only a single sensor wire attached to the neutral point of the machine. Having resolved the stator current into its two components, the flux-producing component can now be adjusted to produce the minimum input power for a fixed amount of output power (fixed speed) by utilizing the converter to control the amplitude of the applied stator voltage.

II. Determination of the Air Gap Flux from the Third-Harmonic Stator Phase Voltage Component

One of the key points in this work is the determination of the instantaneous air gap flux amplitude and its relative position with respect to the stator current vector by utilizing the third harmonic component present in the stator phase voltage. A brief discussion of the machine operating principles is necessary in order to introduce the method of measuring the air gap flux devised in this research.

Induction machines, as the majority of electromagnetic devices, are designed to work in the saturation region of the B-H characteristic of the magnetic material utilized in their construction. The stator current circulating through the quasi-sinusoidal distribution of the windings in the machine stator creates a magnetomotive force (mmf) approximately sinusoidally distributed around the air gap. This quasi-sinusoidal mmf distribution establishes an quasisinusoidal flux density distribution around the air gap. If saturation and the winding harmonics are neglected, then the air gap flux density is sinusoidal and, in particular, if P is the number of poles, then the spatial distribution of flux density in the air gap can be written as

$$B_g(\theta_m) = B_{g1} \sin \frac{P\theta_m}{2} \tag{1}$$

where θ_m is an angular circumferential measure around the air gap.

It is helpful to pause to consider what happens to the air gap flux as the stator teeth begin to saturate. Clearly, the teeth with the highest flux density will saturate first so that the flux density distribution will begin to assume a flattened sinusoidal form with peak value B_{sat} as shown in Fig. 1.

Note that the amplitude of the fundamental component B_{g1} will be somewhat greater than B_{sat}. The flattening of the air gap density is produced primarily by a third-harmonic component that has its origin in the nonlinear magnetic characteristic B-H curve of the magnetic material.

If the machine phases are connected in wye without a neutral connection, no zero sequence current components (triplen harmonics in a three-phase system) will exist. In addition, if the rotor cage is assumed to be equivalent to a delta winding connection, the induction machine can be viewed as an ungrounded three phase wye-delta transformer where no circulation of zero sequence current is possible.

Therefore, the stator currents and, consequently, the air gap mmf will contain only the so-called characteristic harmonics (fifth, seventh, 11th, and so on), whereas the air gap flux and, consequently, the phase voltages contain, in addition, the triplens and high-frequency slot components. The amplitude of these harmonics is a function of the saturation level, which is dictated by the amplitude of the fundamental component. It is necessary at this point to note that the third-harmonic component of the air gap flux will link the stator winding, inducing a third-harmonic stator phase voltage, only if the stator winding distribution function contains a nonzero third-harmonic spatial component. Consequently, the stator winding has to have a pole pitch different of 2/3 in order for the third-harmonic spatial component to exist. Fortunately, 2/3 pole pitch is not common in practice since a machine optimal design dictates a bigger value for the pole pitch that favors a higher flux linkage for the winding. The pole pitch is normally chosen as a value that minimizes but does not eliminate the fifth and the seventh winding space harmonics.

In general, the air gap flux density is also modulated by a high-frequency component due to the existence of stator and rotor slots. Fig. 2 shows a cross-sectional view of the air gap and stator and rotor slots with the variation in the flux density caused by them. This high-frequency component is proportional to the rotor mechanical speed and can be utilized as a means to measure the speed, thereby eliminating the need for a tachometer or an encoder [8].

When the three-phase voltages are summed, the fundamental and characteristic harmonics are cancelled, and the resultant waveform contains mainly a third-harmonic together with high-frequency components due to the rotor slots. This resultant term is produced by the third-harmonic of the air gap flux, which clearly maintains a constant position with respect to the fundamental flux component. Therefore, the third-harmonic component of the zero sequence voltage can be used to locate the instantaneous position of the air gap flux as well as to estimate its fundamental amplitude.

Note that induction of a third harmonic voltage in the

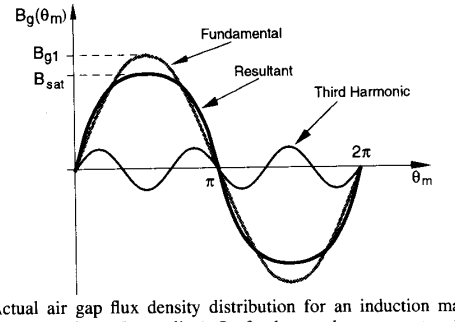

Fig. 1. Actual air gap flux density distribution for an induction machine operating at rated voltage (heavy line). Its fundamental component and third harmonic components are also shown.

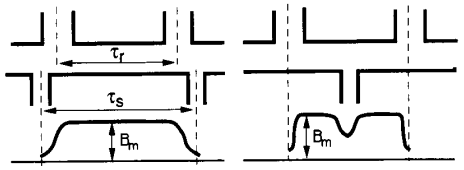

Fig. 2. Illustration of slot flux pulsations showing two limiting alignments of stator and rotor teeth.

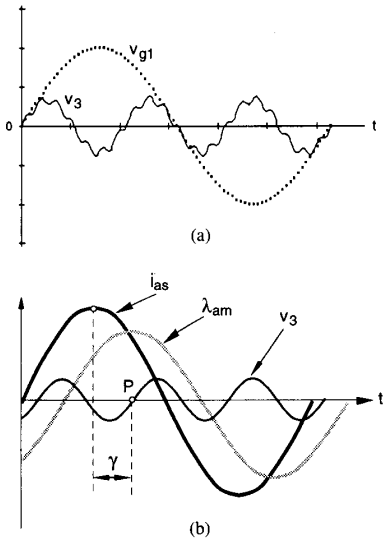

Fig. 3. (a) Fundamental air gap voltage V_{g1} and stator phase voltage third-harmonic component V_3 and (b) fundamental components for the phase current, voltage, and the third harmonic showing the angle displacement γ between the current and third-harmonic component.

stator windings due to stator or rotor currents is also possible. However, for a wye-connected machine without a neutral return, these components can exist only if positive or negative sequence third-harmonic components flow in the stator winding. Summing the three-phase voltages will cancel out these harmonic components in much the same manner as the fundamental. In cases where the machine is delta connected, zero sequence third-harmonic currents can flow around the delta, provided that the winding distribution contains a third-harmonic spatial component. However, in this case, with practical winding patterns, the current is very small, typically a few percent of rated current. In exceptional cases, the severity of the measurement error could, however, prevent use of this measurement technique.

Fig. 3(a) shows typical waveforms of the fundamental air gap voltage and the third harmonic modulated by the rotor slot harmonics, which are obtained after the summation of the stator phase voltages. After eliminating the high-frequency component, which is utilized to measure the rotor mechanical speed, the third harmonic is obtained as shown in Fig. 3(b).

If, for instance, the position of point P (Fig. 3(b)) in the third-harmonic waveform is known with respect to the terminal voltage or current, then the relative position of the fundamental component of the air gap flux is also known with respect to these same terminal variables. In order words, the position of the air gap flux with respect to the terminal current or voltage can be measured at all times if a given point on the third harmonic voltage is located and tracked.

As shown in Fig. 3, the angle γ between the air gap flux and the phase current can also be measured and used to compute the induction machine torque.

III. Efficiency Control of Induction Machine Based on Stator Third-Harmonic Voltage Component

In general, the efficiency of any machine can be obtained from the ratio of the mechanical output to the electrical input power. The output power can be computed from the product of the developed electromagnetic torque and shaft mechanical speed. However, the practicalities of implementation imply regulation of either torque or speed so that the efficiency is maximized indirectly by minimizing the input power. The proposed system for calculating torque utilizes only one additional current sensor for the machine line current. No explicit speed sensor is necessary since the mechanical speed can be calculated from the high-frequency signal modulating the third-harmonic component. This signal originates from the air gap flux modulation introduced by the rotor slots. The frequency of this signal ω_{slot} is a function of the number of rotor slots n_s, the rotor speed ω_r, and the synchronous frequency ω_e, according to (2):

$$\omega_{slot} = (n_r\omega_r \pm \omega_e). \tag{2}$$

The frequency of the rotor slot pulsations ω_{slot} is detected as described in [8], and the rotor mechanical speed is readily computed from it.

Two implementation methods are proposed for the efficiency controller. In the first method, the amplitude of the third-harmonic component is not used. However, the phase of the signal is employed to resolve the stator current into the flux- and torque-producing components. The amplitude and frequency of the inverter are then adjusted to reach a minimum input power by adjusting the flux-producing component of motor current while keeping the speed constant, as shown in Fig. 4. In general, the efficiency controller operates only in the background with the minimization algorithm updating the voltage and frequency commands only several times per second to drive the operating point to a minimum input power while keeping the output power constant. Hence, the

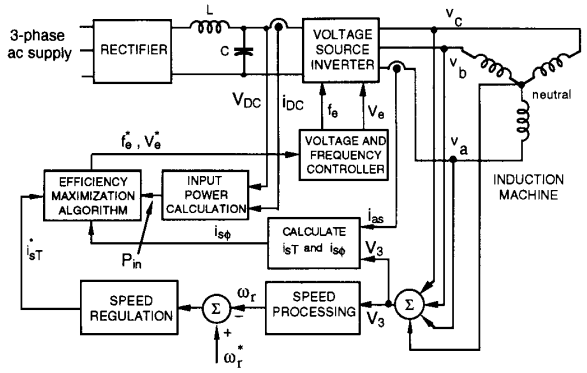

Fig. 4. Simplified diagram for the first method proposed for the efficiency controller. i_{sT}, $i_{s\phi}$ are the torque- and flux-producing components of the stator current, respectively.

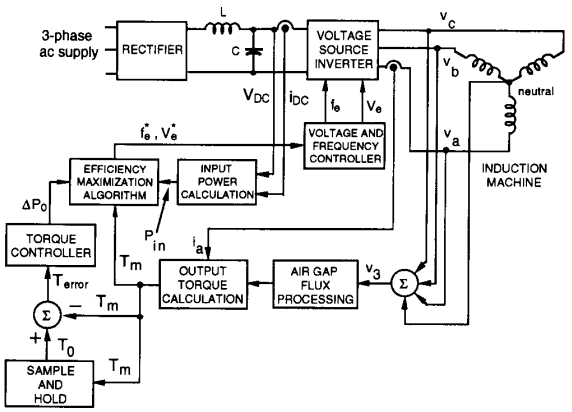

Fig. 5. Control block diagram for the second method proposed for the efficiency maximizer utilizing torque control.

overall dynamic response of the drive remains essentially unaffected. Care must, of course, be taken to disable the optimum controller when a new speed command is issued or when the load demand changes. However, such problems have sensibly been resolved in [7]. If the torque is reasonably constant with speed or varies only slowly, a maximum efficiency condition can still be maintained even while the torque is changing.

A second control method is possible in cases where the torque speed curve is essentially fixed, such as fans and pumps. In such cases, the speed measurement can be dispensed with since regulation at constant torque implies that output power is also maintained constant. Fig. 5 shows the implementation for this efficiency control strategy.

The torque is now computed from the stator current and air gap flux as shown in (3).

$$T_e = \frac{3P}{4} |i_{as}| \, |\lambda_g| \sin\gamma \tag{3}$$

where $|i_{as}|$ and $|\lambda_g|$ are the absolute values of the phase current and air gap flux, respectively, and P is the number of poles. The argument defined as γ represents the phase displacement between the current and the fundamental component of the air gap flux. In (3)

$$\lambda_g = \int v_g \, dt \tag{4}$$

where v_g is the fundamental component of the air gap voltage and

$$v_g = f(v_3). \tag{5}$$

Equation (5) describes the functional dependance of the fundamental component of the air gap voltage on the amplitude of the third harmonic.

Alternatively, T_e can be computed from

$$T_e = \frac{3P}{4} \frac{|i_{as}| \, |v_g|}{\omega_e} \cos\gamma \tag{6}$$

where ω_e is the desired angular frequency commanded to the inverter.

IV. Experimental Results

Fig. 6(a) shows the third-harmonic voltage waveform and one of the phase currents for the test induction machine (7.5 hp, 230 V, four poles; refer to Appendix) obtained experimentally for rated load condition and sinusoidal voltage supply.

A spectrum analyzer is utilized to measure the harmonic contents of the third harmonic, which is shown in Fig. 6(b). As predicted, the third harmonic is clearly the dominant component, followed by the rotor slot harmonic. The amplitude of the third-harmonic signal is a function of the saturation level of the machine and, consequently, a function of the excitation voltage.

Fig. 7 presents experimental results showing the variation of the sensed third-harmonic rms voltage V_3 with the fundamental rms line voltage V_{l1} for a sinusoidal excitation at no load. It can be noted that a very useful signal for the third-harmonic voltage is present even for excitation voltages approaching 30% of the rated value.

As the machine mechanical load increases, the angle between fixed points in the third-harmonic voltage waveform and the line current increases as expected. Fig. 8 shows this variation for the case where the machine is loaded from zero to rated load, keeping the stator voltage at rated value.

The motor output power is computed from the third-harmonic signal where the third harmonic itself gives us information about the air gap flux while the slot harmonic is used to estimate the mechanical speed. Table I shows the experimental and estimated results obtained for the test machine. The torque estimate $T_m est$ is computed from (3)–(5). The function relating the third-harmonic amplitude and the air gap voltage expressed by (5) is derived from the experimental results presented in Fig. 7. The speed estimation $\omega_r est$ is attained from the rotor slot ripple as mentioned above.

The results in Table I demonstrate that the estimated values are very close to the actual measured values showing that the third-harmonic signal is very suitable to estimate the machine speed, torque, and output power. Fig. 9 shows the measured and estimated motor torque as a function of the speed for a

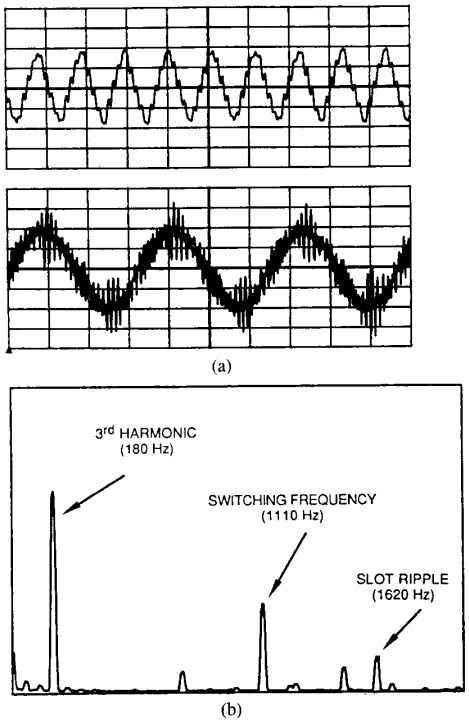

Fig. 6. Experimental results obtained for the test motor driven by a PWM voltage source inverter: (a) Line current (bottom trace: 5 A/div) and stator third-harmonic voltage (upper trace: 5 V/div); (b) third-harmonic voltage spectrum (full scale of 15 V).

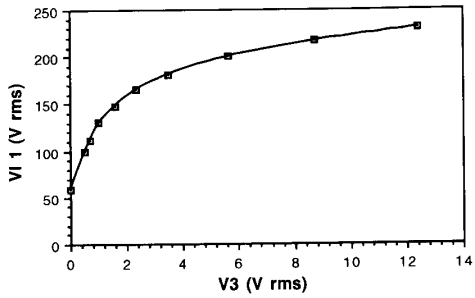

Fig. 7. Experimental results showing the dependence of the third-harmonic voltage component on the fundamental value of the applied line voltage for the test machine at no load.

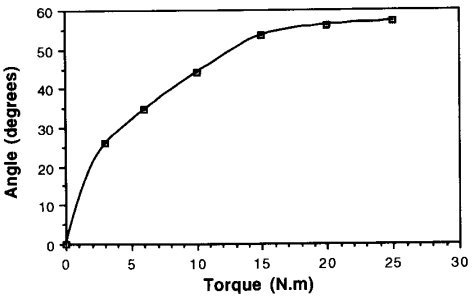

Fig. 8. Angular displacement between the air gap flux and line current measured from the third-harmonic component as a function of torque for the test machine operating at rated voltage.

TABLE I
EXPERIMENTAL AND ESTIMATED RESULTS OBTAINED FROM THE THIRD-HARMONIC VOLTAGE SIGNAL FOR THE TEST MACHINE

P_{in} (W)	T_m (N · m)	ω_r (r/min)	P_o (W)	effic.	T_m est. (N · m)	ω_r est. (r/min)	P_o est. (W)	effic. est
6613.00	29.82	1744.30	5447.01	0.82	29.80	1740.28	5430.80	0.82
5673.00	25.56	1753.00	4692.16	0.83	26.17	1750.99	4799.43	0.85
5049.00	22.72	1758.70	4184.37	0.83	22.95	1756.34	4220.18	0.84
4433.00	19.88	1764.10	3672.56	0.83	20.08	1761.70	3704.56	0.84
3816.00	17.04	1770.30	3158.97	0.83	17.32	1767.05	3204.18	0.84
3227.00	14.20	1775.20	2639.77	0.82	14.54	1772.41	2699.47	0.84
2693.00	11.36	1779.80	2117.28	0.79	12.09	1777.76	2251.18	0.84
2120.00	8.52	1784.50	1592.16	0.75	9.08	1783.12	1696.00	0.80
1559.00	5.68	1789.00	1064.11	0.68	5.69	1788.47	1064.74	0.68
994.00	2.84	1793.30	533.34	0.54	3.32	1792.04	622.91	0.63
479.00	0.00	1797.40	0.00	0.00	0.00	1797.39	0.00	0.00

constant frequency of 60 Hz and rated voltage of 230 V. Very good correlation is clearly obtained.

Fig. 10 shows the motor input power P_{in} as a function of the stator line voltage. From it, one can verify the savings of electrical input power that can be achieved as a function of the fundamental component of the applied line voltage for the test motor operating at relatively low torque and medium speed (0.6 pu speed and 0.2 pu load torque). The results shown in Fig. 10 were obtained from a experimental procedure where the input power P_{in} is measured by a digital wattmeter while the motor mechanical output power, which is estimated from the third-harmonic signal, is kept constant. Fig. 11 shows the experimental results relating an increase in

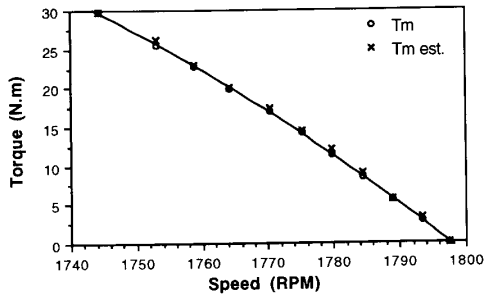

Fig. 9. Measured and estimated mechanical load torque versus speed.

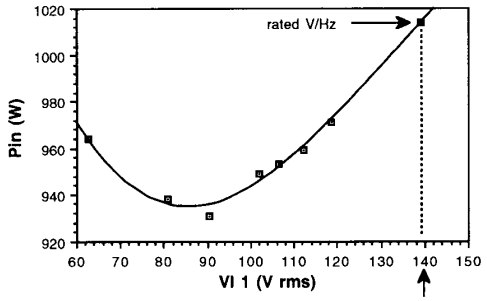

Fig. 10. Experimental results showing the reduction in input power when the machine is operated at reduced voltage. Results obtained for the test machine operating at 0.6 pu speed and 0.2 pu load torque.

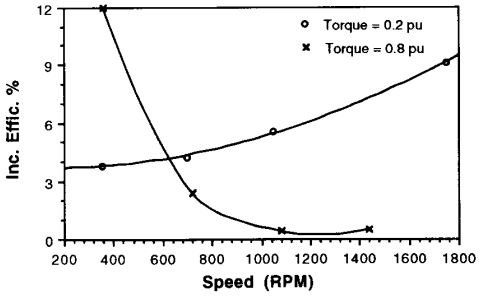

Fig. 11. Efficiency increase with respect to the maximum machine efficiency as a function of rotor speed at load torques of 0.8 and 0.2 pu.

machine efficiency as a function of speed for both relatively heavy and light torque loads of 0.8 and 0.2 pu, respectively.

The efficiency increase is computed with reference to the efficiency obtained when the machine is operating at the same load torque with rated volts per hertz. It can be noted that when the motor is heavily loaded, efficiency is improved primarily for low-speed operation, whereas for light loads, efficiency improvement is primarily obtained at high speeds due to the change in the optimum balance in iron and copper losses for the two load conditions. Note that a very substantial increase in efficiency can be achieved at high speeds and low torque, suggesting that good induction motor efficiencies can be maintained over a wide speed range.

V. Conclusion

A new simple and low-cost method of efficiency maximization that involves sensing of the third-harmonic component of the air gap flux has been presented. It is shown that a predominant third-harmonic voltage component is obtained when the three stator phase voltages are summed. This third-harmonic component can then be used to determine the resulting instantaneous position of the fundamental component of the air gap flux. A high-frequency signal, which is produced by the variation of air gap reluctance due to stator and rotor teeth, modulates the third-harmonic component and can be used as a means to measure the rotor speed. The efficiency controller computes the output power by calculating torque from air gap flux and current and measuring the rotor speed from the third-harmonic signal. The input dc link power is also computed, and the efficiency of the drive system is maximized by means of a control optimization algorithm. Experimental results were presented, demonstrating measurement of the third-harmonic voltage component and verifying the dependance of torque with the angle between air gap flux and stator current as resolved via the third harmonic.

In closing, it is clear that the utilization of the third-harmonic signal to locate the air gap flux can also be utilized in other applications besides maximization of efficiency. Presently, research is now being carried out on a field-oriented induction machine drive system where this signal is used to implement an adaptive control for corrections in the slip frequency calculation in order to avoid the effects due to detuning caused by deviations in the estimated values for rotor resistance, leakage, and magnetizing inductances. In addition, a new and simple direct torque control scheme that utilizes this third-harmonic component is under investigation.

TABLE II
Induction Machine Ratings and Parameters

Quantity	Symbol	Value
Line voltage	VI	230 V rms
Output power	P_o	7.5 hp
Speed	ω_r	1750 r/min
Poles	P	4
Stator resistance	r_s	0.210 Ω
Rotor resistance	r_r	0.193 Ω
Stator leakage reactance	X_{ls}	0.698 Ω
Rotor leakage reactance	X_{lr}	0.698 Ω
Unsaturated magnetizing reactance	X_m	16.95 Ω
Number of rotor slots	n_r	38

Appendix

Table II shows the ratings and parameters of the induction machine used to obtain the experimental results presented before.

References

[1] A. D. Little Inc., "Energy efficiency and electric motors," Final Rep. Fed. Energy Admin., Washington, DC, Contract C0-0450217-00, May 1976.

[2] ____, "Classification and evaluation of electrical motors and pumps," Final Rep. Energy Environ. Sys. Div., Argonne Nat. Lab., Argonne IL, Contract 31-109-98-5084, Feb. 1980.

[3] T. M. Rowan and T. A. Lipo, "A quantitative analysis of induction motor performance by SCR voltage control," *IEEE Trans. Industry Applications*, vol. IA-19, no. 4, pp. 545–553, July/Aug. 1983.

[4] F. J. Nola, "Power factor control systems for ac induction motor," U.S. Patent 4 052 648, Oct. 4, 1977.

[5] N. Hingorani, "Power electronics: A national priority," "Sealed in silicon: The power electronics revolution," Electric Power Res. Inst., *EPRI J.*, Reprint, Dec. 1986.

[6] D. S. Kirschen, "Optimal efficiency control of induction machines," Ph.D. thesis, Univ. Wisconsin-Madison, 1985.

[7] D. S. Kirschen, D. W. Novotny, and T. A. Lipo, "On-line efficiency optimization of a variable frequency induction motor drive," *IEEE Trans. Industry Applications*, vol. IA-21, pp. 610–616, May/June 1985.

[8] D. Zinger, F. Profumo, T. A. Lipo, and D. W. Novotny, "A direct field oriented controller for induction motor drives using tapped stator windings," *IEEE Trans. Power Electron.*, vol. 5, no. 4, pp. 446–453, Oct. 1990.

Julio C. Moreira (S'81-M'90) was born in Sao Paulo, Brazil. He received the B.E.E. and M.E.E. degrees in 1979 and 1983, respectively, from the State University of Campinas (UNICAMP). He received the Ph.D. degree in electrical engineering from the University of Wisconsin, Madison, in 1990.

He worked as an Engineer and later as a Vice Coordinator of the Electric Drive Systems Research Laboratory at UNICAMP from 1980 to 1985. In 1981, he became a Researcher and an Assistant Professor at that same institution, teaching courses in electrical machines, power electronics, and controls. His research activities included the development of dc and ac motor drives for an electric vehicle. He also served as a consultant in the areas of electric drive systems and switched power supplies. He later joined the Whirlpool Corporate Research and Engineering Center, Benton Harbor, MI, where he is involved with research in the areas of power electronics, electric drive systems, controls, and motor design.

Dr. Moreira is a member of ETA NOΣ, IAS, PES, and IES.

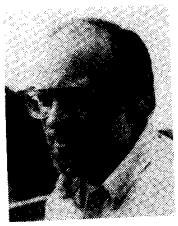

Thomas A. Lipo (M'64-SM'71-F'87) received the B.E.E. and M.S.E.E. degrees from Marquette University, Milwaukee, WI, in 1962 and 1964, respectively, and the Ph.D. degree in electrical engineering from the University of Wisconsin in 1968. He was an NRC Postdoctoral Fellow at the University of Manchester Institute of Science and Technology, Manchester, England, from 1968 to 1969.

From 1969 to 1979, he was an Electrical Engineer in the Power Electronics Laboratory of Corporate Research and Development of the General Electric Company, Schenectady, NY. He became Professor of Electrical Engineering at Purdue University, Lafayette, IN, in 1979 and later joined the University of Wisconsin, Madison, in the same capacity. He has been involved in the research of power electronics and ac drives for over 25 years.

Dr. Lipo has received 11 IEEE prize paper awards including corecipient of the Best Paper Award in IEEE TRANSACTIONS ON INDUSTRY APPLICATIONS for 1984. In 1986, he received the Outstanding Achievement Award from the IEEE Industry Applications Society for his contributions to the field of ac drives.

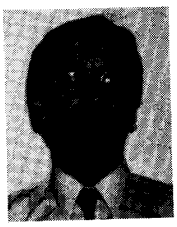

Vladimir Blasko was born in Klenovnilk, Yugoslavia, on December 14, 1953. He received the B.Sc., M.Sc., and Ph.D. degrees in electrotechnical engineering from Electrotechnical Faculty of Zagreb, Yugoslavia, in 1976, 1982, and 1986, respectively. For his Ph.D thesis, he received the "Vatroslav Bednjanic" award in 1987.

From 1976 to 1988, he worked at the Electrotechnical Institute Rade Koncar, Zagreb, in the Power Electronics and Automatic Control Department. He was mainly involved with the research, development, and design of the drives for electrical vehicles with high current transistor converters. During the academic year 1988/1989, he was at the University of Wisconsin, Madison, as a recipient of the IREX scholarship. He worked on research of new vector control strategies of induction motors and on the development of the modified C-damp converter for switched reluctance motors. Since September 1989, he has been with the Research and Development Center of the Otis Elevator Company, Farmington, CT. He has been working on the research, development, and design of high-performance ac elevator drives. His primary areas of interest are in ac drives, power electronics circuits, and control techniques.